World Academy of Science, Engineering and Technology
International Journal of Mechanical and Mechatronics Engineering
Vol:2, No:4, 2008

Fluid Flow Analysis and Design of a Flow Distributor in a Domestic Gas Boiler Using a Commercial CFD Software

Lukasz Peronski, Roy Bratley, Derek B. Ingham, Lin Ma, Mohamed Pourkashanian, and Stephen Taylor

***Abstract*—**The aim of the study was to investigate the possible use of commercial Computational Fluid Dynamics (CFD) software in the design process of a domestic gas boiler. Because of the limited computational resources some simplifications had to be made in order to contribute to the design in a reasonable timescale.

The porous media model was used in order to simulate the influence of the pressure drop characteristic of particular elements of a heat transfer system on the water-flow distribution in the system. Further, a combination of CFD analyses and spread sheet calculations was used in order to solve the flow distribution problem.

***Keywords*—**CFD, domestic gas boilers, flow distribution, heat exchanger, porous media

I. Introduction

HEAT transfer in compact heat exchangers has been investigated for many years. Many formulae based on experimental data regarding various geometries and conditions are available in the literature [4], [5], [6]. However the use of these formulae is limited to geometries and operating conditions under which the experiments were performed. There is often a need to predict the performance of unconventional heat exchange systems and this is very difficult. Reliance on engineering experience, intuition and tests of prototypes are common industrial practice. Therefore Computational Fluid Dynamics (CFD) codes are potentially very useful in design processes as they are designed to predict all important heat transfer parameters, i.e. flow and temperature fields as well as heat transfer performance for arbitrary geometry and flow conditions. As CFD codes provide such extensive information it may significantly reduce the number of experiments needed to launch a new product and decrease the cost as well as the timescale of a design process of heat exchange systems.

Unfortunately CFD has limitations. One of them is the requirement of a large computational power demand. Either large clusters of workstations or multiprocessor machines are often needed to analyse real industrial problems. It is a difficulty especially for small companies with limited computational resources, such as the one where this research was conducted. In order to overcome this difficulty, some simplifications and complementary tools must be used in order to reduce the computational resources required.

It is a common CFD practice to analyse some small repeatable elements of a heat exchanger, see [7] - [10]. However, even in heat exchangers with repeatable geometrical entities, the fluid velocities are often not the same in all the repeatable domains because of the maldistribution which affects the heat transfer. Therefore ideally a fluid flow and heat transfer analysis of the entire heat transfer system should be performed in order to fully understand the problems related to the performance of the system. Unfortunately a direct CFD simulation of the heat transfer in complex heat exchangers requires large computational resources.

Procedures based on experimental formulae have been used for many years and they do not have to be replaced but can possibly be complimented by CFD. Therefore some parameters related to the operation of heat exchangers could be analysed by means of CFD codes and others by traditional methods.

There are problems in a design process of heat exchangers which can especially be complemented by a CFD analysis. Fluid flow distribution analysis is one of them. As the heat transfer and temperature field in heat exchangers strongly depends on the fluid flow, the CFD fluid flow analysis may provide crucial information for traditional heat transfer calculations. Quite often a uniform flow distribution is a design assumption and CFD can be a tool to investigate if such an assumption is correct and to design an appropriate flow distributor if necessary.

As stated in [3], a fluid flow distribution problem can be solved simply by the introduction of an additional flow resistance by means of a flow restrictive device (e.g. perforated plate, perforated tube or other screen). However an

L. Peronski is with Enertek International Ltd.; 1 Malmo Road; Hull; HU7 0YF (phone: (0044) 1482 877 500; e-mail: lukaszperonski@enertek.co.uk) and with The University of Leeds; School of Process, Environmental and Materials Engineering; CFD Centre; Leeds; LS2 9JT; UK (e-mail: mat4l2p@leeds.ac.uk).

D. B. Ingham, M. Pourkashanian and L. Ma are with The University of Leeds; School of Process, Environmental and Materials Engineering; CFD Centre; Leeds; LS2 9JT; UK.

S. Taylor and R. Bratley are with Enertek International Ltd.; 1 Malmo Road; Hull; HU7 0YF (phone: (0044) 1482 877 500; e-mail: info@enertek.co.uk)

effective screen may increase a pressure drop significantly. In the example presented in [3] (perforated pipe distributor) the pressure drop over the holes in the pipe must be about 10 times the pressure variations causing the maldistribution in the system (the inlet velocity head or the pressure drop over the length of the pipe) in order to decrease the maldistribution to 5%. As CFD can evaluate the pressure drop for an arbitrary geometry, it can be used to determine changes to a design which would differentiate the pressure drop between particular elements of a system in a way which would impose an appropriate flow distribution. When the introduction of a screen is technically simpler than a modification of existing elements of a system, CFD can be used to design either a non-uniform screen or a distributor which would impose an appropriate pressure drop in locations where it is needed. Such a solution would result in a lower overall pressure drop than with a uniform distributing screen.

In this work a porous media model in flow distribution problems, as well as combined CFD and spread sheet calculations, were used for a design of a distributor.

II. Description of the Problem

The heat exchanger under investigation is designed for domestic gas central heating boilers. It is capable of working in a fully condensing mode. The thermal energy of the combustion gases is transferred in the heat exchanger into the central heating water circuit in order to be eventually transferred to the air in rooms by means of radiators.

The heat exchanger consists of identical repeatable castings (also referred to as sections) assembled together. Only the front and rear sections are slightly different. The waterway geometry of the single casting is presented in Fig. 1. The single casting is designed to the 10 kW heat load and the number of castings in the assembly may vary depending on the required nominal heat load of the assembly. As the castings are symmetrical, only the left hand side of the casting was analysed (see Fig. 2). The same applies to the assemblies as they are symmetrical in the same manner (see Fig. 3).

The aim of this work was to analyse the water distribution between sections of the 4 section assembly as well as the 8 section assembly and to design a distributor if necessary. As shown in Fig. 3, the water enters the assembly at the bottom of the front casting. In the front section the stream of the water splits. Part of the stream flows upwards through the casting while the second part of the stream flows in the horizontal direction and enters the second casting. The water entering the second casting also splits. Part of the water flows upwards through the casting while the rest of the water flows to the next casting and so on. As the flow rate of the water affects the heat transfer and temperature field in the castings, it is important to ensure that there is a uniform flow distribution of water between the castings. This is necessary in order to ensure a high efficiency of the heat exchanger and to eliminate the danger of local boiling of the water.

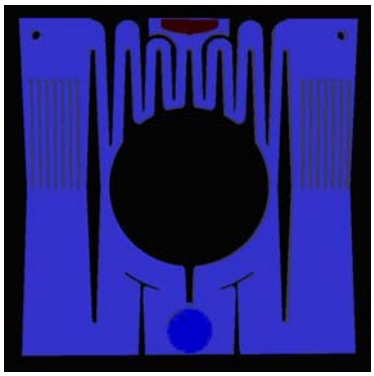

Fig. 1 Waterway of the single casting of the heat exchanger

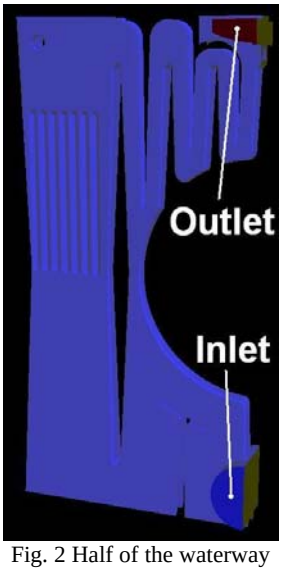

Fig. 2 Half of the waterway of the heat exchanger

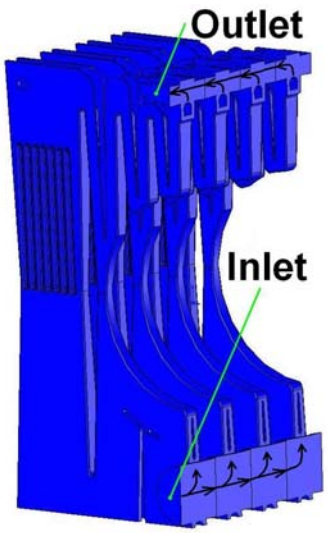

Fig. 3 Geometry of the model of the 4 section heat exchanger assembly

III. Numerical Approach

Before analysing the flow distribution between the sections of the heat exchanger, the numerical model of a single casting was created. As the sections of the assembly are identical (apart from the front and the rear one) a numerical mesh of a single casting could be created and then copied in order to create a model of an assembly. Two alternative meshes were created: with 36 000 cells and 3.7 millions cells. The finer mesh of the model of a single casting is presented in Fig. 4.

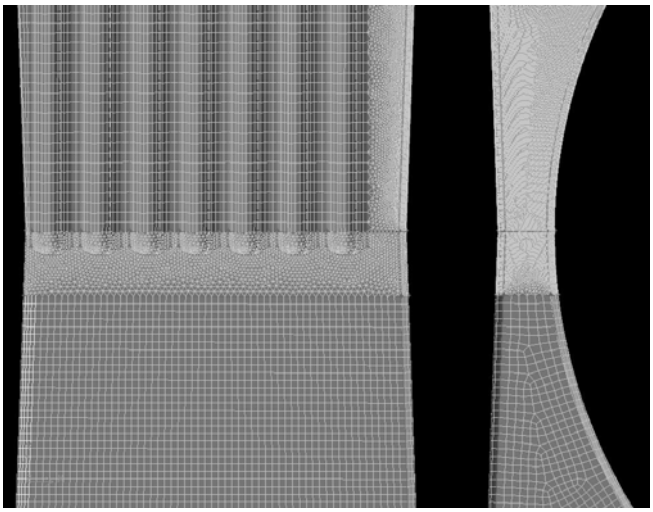

(a)

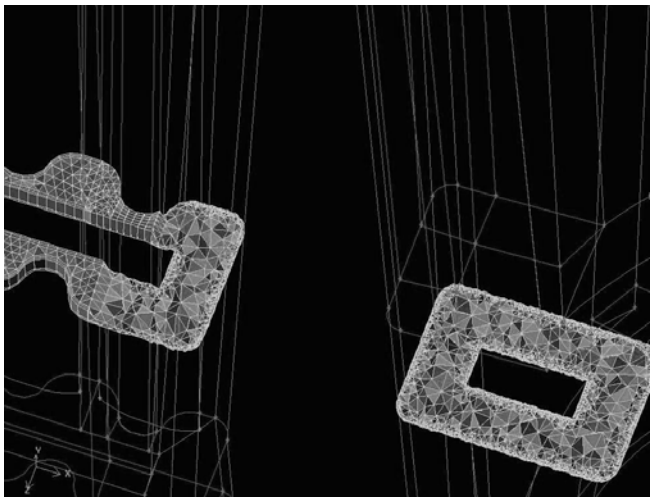

(b)

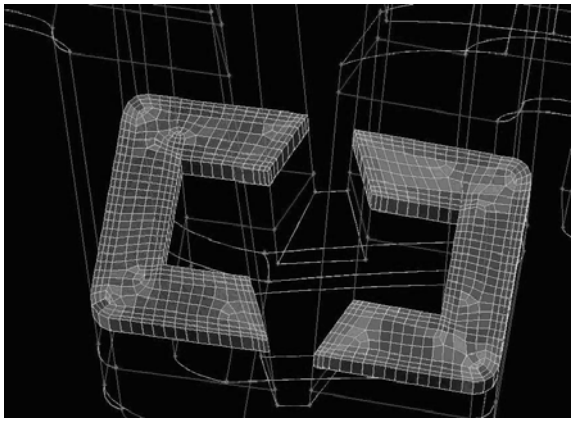

(c)

Fig. 4 Mesh of the water channels of the heat exchanger

Gambit 2.2.30 was used for the preparation of the numerical mesh and Fluent 6.2.16 was used as the solver.

The flow of the water through the single section was modelled for various flow rates and the modelled pressure drop characteristic was compared to the measured one. In order to measure the pressure drop of the water in the single section of the heat exchanger, a mercury manometer was connected to the inlet and outlet pipes. The flow rate of the water was measured by means of a rotameter. The comparison between measured and modelled pressure drop characteristic is shown in Fig. 5.

The resolution of the manometer and therefore the assumed tolerance of the pressure drop readings was 0.02 mH_2O. Further, the calculated uncertainty of the flow measurement was between 0.28 and 0.34 l/min (it was different for different flow rates).

Although there was no significant difference between the pressure drops predicted by the two models (see Fig. 5), the finer mesh was selected for the analysis as it was believed to give more insight into the velocity field of the water. There was only one numerical cell in the coarse mesh between the walls of the narrow channels, and therefore an accurate prediction of the velocity profiles could not be expected from this model.

As the geometry along the waterways in the heat exchanger changes, the velocity of the water as well as the Re number changes too. The expected maximum Re number in the castings of the heat exchanger for nominal operating conditions is about 6000 and therefore transitional flow was expected in the heat exchanger. As shown in Fig. 5, the simulation of the water flow in the single casting of the heat exchanger using the laminar flow model produced a very similar pressure drop to that produced using the k-omega turbulence model.

The flow in the heat exchanger is transitional and it was not certain if laminar or turbulent flow model would give better predictions. Therefore the laminar model was used in this work as it produces results much quicker.

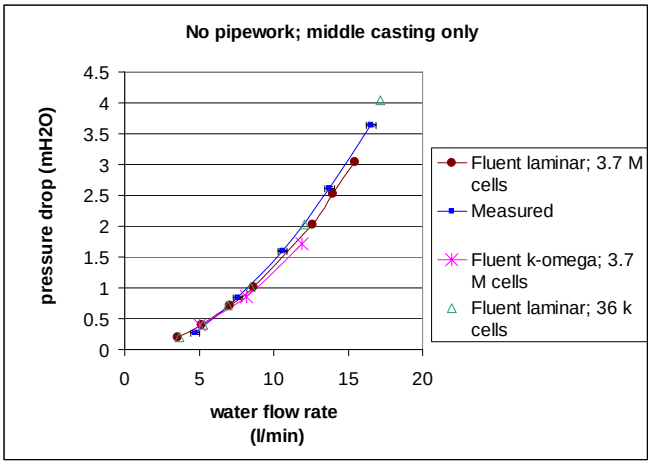

Fig. 5 Measured and calculated pressure drop in the single casting of the heat exchanger

IV. Water-Flow in the Entire Assembly

The water-flow distribution analysis was performed for 4 and 8 section assemblies.

The analysis of the 4 section assembly with the use of the finer mesh (see Fig. 4) would require 4 times more memory (RAM) than the analysis of the single section and therefore was not possible because of the limited computational resources. On the other hand, it was not certain that the coarse mesh would be able to model the flow distribution correctly.

Therefore some simplifications were needed in order to make the analysis of the entire assembly possible. The geometry of the waterway of the single casting was simplified, as shown in Fig. 7. Channel A shown in Fig. 6 was removed as the flow-rate through the channel was relatively low and its effect on the pressure drop characteristic of the entire section was expected to be negligible.

The channel between the locations shown in Fig. 6 referred to as "pressure_bottom" and "pressure_top" was also removed and the remaining parts of the waterway were merged together (see Fig. 7). Then the simplified waterway was meshed and duplicated and the duplicates were merged together (see Fig. 8) in order to create the model of the water-flow of the 4 section assembly. The pressure drop characteristic of the channel between the "pressure_bottom" and "pressure_top" $\Delta p = f(v)$ was read from the model of the single casting (for various flow rates) and it was applied to the simplified waterways by means of the thin porous media regions shown in Fig. 8

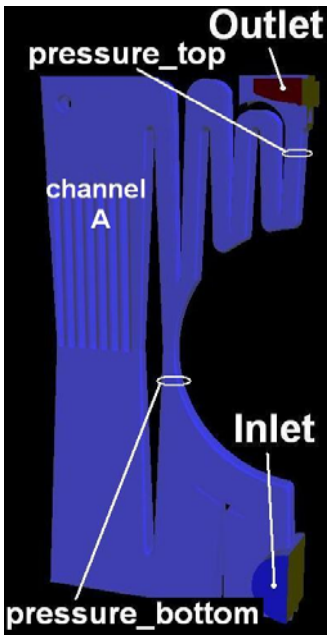

Fig. 6 Original model of the waterway of single section of the heat exchanger

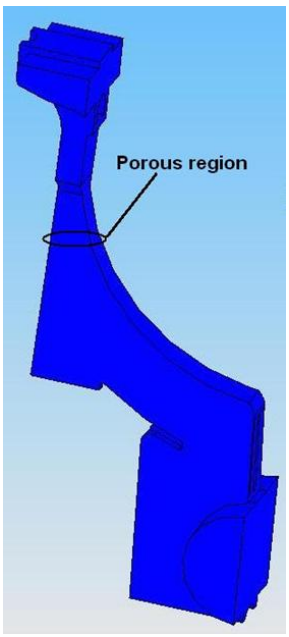

Fig. 7 Simplified model of the waterway of single section of the heat exchanger

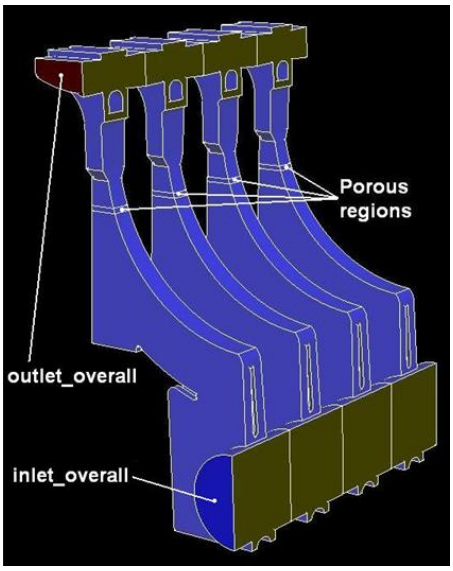

Fig. 8 Model of the waterway of 4 section assembly of the heat exchanger

The porous media characteristics were derived as follows:

The dependence between v and Δp in the channel between "pressure_bottom" and "pressure_top" was read from the model of a single casting and approximated by means of a second-order polynomial function (using MS Excel). The following function was found:

$$\Delta p = 13500v^2 + 0 \cdot v \tag{1}$$

where: Δp - Pressure drop; Pa

v - Velocity of the water in the porous region; $\frac{m}{s}$

The velocity of the water was defined as:

$$v = \frac{\dot{m}}{A \cdot \rho} \tag{2}$$

where $\dot{m}$ is the mass flow rate of the water flowing through the half of the section of the heat exchanger, A is the horizontal cross-sectional area of the porous region, and ρ is the mass density of the water.

Equation (1) implies that the unit of the constant of proportionality is $\frac{kg}{m^3}$ and therefore:

$$\Delta p = 13500 \frac{kg}{m^3} \cdot v^2 \tag{3}$$

The simplified momentum equation for the homogeneous porous media can be written as [11]:

$$\nabla p = S_i \tag{4}$$

where S_i is the source term for the momentum equation in the i direction.

As stated in [11], (4) can be written for a particular direction as:

$$\Delta p = -S_i \cdot \Delta n \tag{5}$$

The momentum source term S_i for the porous media is defined as follows [11]:

$$S_i = -\left(C_2 \cdot \frac{1}{2} \cdot \rho \cdot v_i^2 + \frac{\mu}{\alpha} \cdot v_i \right) \tag{6}$$

and therefore:

$$\Delta p = \left(C_2 \cdot \frac{1}{2} \cdot \rho \cdot v_i^2 + \frac{\mu}{\alpha} \cdot v_i \right) \cdot \Delta n \tag{7}$$

$$\Delta p = C_2 \cdot \frac{1}{2} \cdot \rho \cdot \Delta n \cdot v_i^2 + \frac{\mu}{\alpha} \cdot \Delta n \cdot v_i \tag{8}$$

The comparison of (3) with (8) gives:

$$\frac{\mu}{\alpha} \cdot \Delta n \cdot v_i = 0 \tag{9}$$

$$C_2 \cdot \frac{1}{2} \cdot \rho \cdot \Delta n = 13500 \frac{kg}{m^3} \tag{10}$$

Therefore the viscous resistance factor:

$$\frac{1}{\alpha} = 0$$

The inertial resistance factor C_2 is given by:

$$C_2 = \frac{2 \cdot 13500 \frac{kg}{m^3}}{\rho \cdot \Delta n} = \frac{2 \cdot 13500 \frac{kg}{m^3}}{998 \frac{kg}{m^3} \cdot 0.002 m} = 13527 \frac{1}{m} \tag{11}$$

where:

ρ - Mass density of the water; $\frac{kg}{m^3}$

Δn - Thickness of the porous region in the model; m

μ - Dynamic viscosity; $\frac{kg}{m \cdot s}$

The resistance factor was used as an input data for Fluent porous media model and Fluent 6.2.16 was used as the solver with the laminar flow model.

The mass flow rate through the front section (see Fig. 8) was less than 4.3 % higher than through the rear one for the range of flow rates through the entire assembly from 0.37 to 1.68 kg/s. Based on these results, the decision was made that the flow distribution is acceptable and there is no need for a flow distribution device.

V. Distributing Tube for Large (8 Section) Appliances

The previous analysis (see paragraph IV) indicated that the distribution of the water between the sections of the 4 section version of the heat exchanger was almost uniform.

However the same analysis done for the 8 section version (not shown here) gave a 20% difference in the flow-rate of the water through the first and the last sections.

Fig. 9 and Fig. 10 illustrate the way that the water flows through the 8 section heat exchanger. The water enters the appliance through the "Water inlet". The stream of the inflowing water splits in the section 1 (at the point 3). Part of it flows upwards while the rest of the stream flows into the next section. The streams of the water entering the other sections (at the points 5, 7, 9, 11, 13, 15) split in the same manner. Part of inflowing water flows upwards while the rest of the stream flows horizontally and enters the next section. As section 8 is the last one then all the water entering this section flows upwards. All the streams of the water flowing upwards flow in parallel through the sections of the heat exchanger and join together at the top horizontal channel. Next the water exits the heat exchanger through the "Water outlet".

There may be two possible reasons for the non-uniform distribution of the water-flow between the sections:

(i)The flow resistance characteristic between the "Water inlet" and "Water outlet" may be different for different streams depending on which casting they flow through. It is because the distance from the inlet and outlet and each particular section is different. Moreover the flow-rate changes along the bottom and top horizontal channel so the flow resistance changes.

(ii) The momentum of the water entering the assembly can make the water flow through the right hand side sections rather than the left hand side sections of the assembly (see Fig. 9).

In order to ensure uniform water flow distribution between all sections of the assembly it was decided to use a distributing tube.

The distributing tube would be a perforated tube inside the bottom horizontal channel of the appliance (see Fig. 10 and Fig. 11). The diameter of holes in the tube and consequently flow resistance would vary in the way that would ensure uniform flow distribution of the water between sections (the diameter of holes in Fig. 11 is uniform, but it is not in the final design).

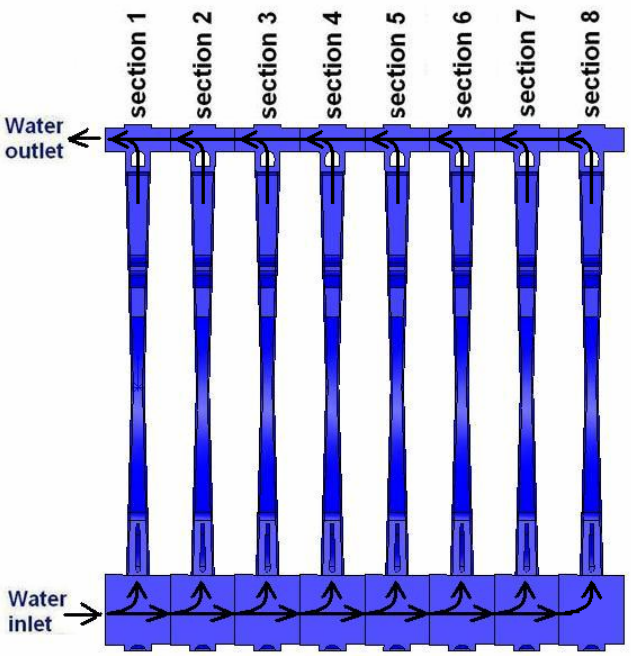

Fig. 9 Cross-section view of the 8 section heat exchanger

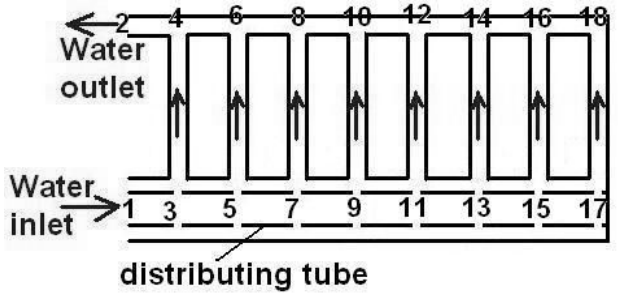

Fig. 10 Diagram of the water distribution between sections of the 8 section version of the heat exchanger

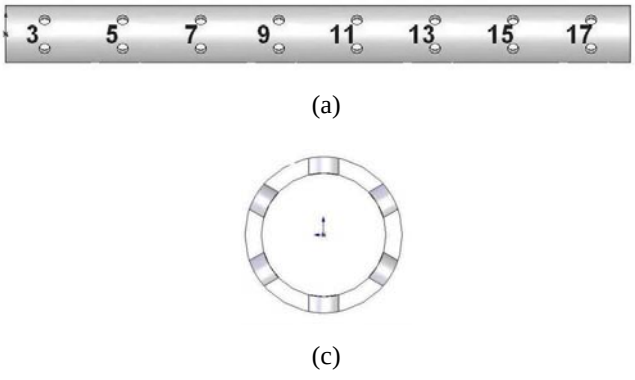

Fig. 11 Distributing tube (a) side view; (b) cross-sectional view

The points where the streams of water split (at the bottom of the assembly) or join (at the top of the assembly) are denoted by numbers 3 ÷ 16 (see Fig. 10) and this gives the possibility to denote the straight channels between them by means of two numbers. They are the channels of fixed flow rate.

The horizontal channels at the bottom and the top of the heat exchanger have uniform cross-section area. All sections of the assembly (vertical channels) are the same apart from the section 1 and section 8 (channel 3-4 and 17-18 in Fig. 10). Section 1 and section 8 were designed for ½ flow rate of inner section. Because of lack of characteristics of pressure drop of the left and right hand side sections the following assumptions were made:

(i) Holes in the distributing tube in section 1 (channel 3-4) are the same as in section 2 (channel 5-6).

(ii) Holes in the distributing tube in section 8 (channel 17-18) are the same as in section 7 (channel 15-16).

Also other simplifying assumptions were made:

(iii) The diameter of holes in the distributing tube in the rest of the sections (point 5, 7, 9, 11, 13 and 15 in Fig. 10 and Fig. 11) should be diverse so that the flow rate through each of them would be the same.

(iv) There are six holes with the same diameter around the distributing tube at each point which refer to a particular section of the heat exchanger assembly (see Fig. 10 and Fig. 11).

The velocity of the water entering the assembly was calculated from the known mass flow rate (known operating conditions of the boiler),

$$v_1 = \frac{\dot{m}_1}{A_1 \cdot \rho} \tag{12}$$

The velocity of the water in the vertical channels is shown in Fig. 10 and were calculated from the mass balance using the assumption that the mass flow rate through each of the inner sections (channel 5-6; 7-8; 9-10; 11-12; 13-14; 15-16) is the same and the flow rate through the front and the rear sections is half of the flow rate through one inner section. The mass density of the water ρ was assumed to be constant. These assumptions lead to the following equations:

(i) Velocities in the vertical channels:

$$v_{5-6} = v_{7-8} = v_{9-10} = v_{11-12} = v_{13-14} = \\ = v_{15-16} = \frac{v_{3-5} \cdot A_{1-3}}{A_{5-6} \cdot (n_f + 0.5)} \tag{13}$$

(ii) Velocities in the horizontal channels:

$$v_{3-5} \cdot A_{3-5} \cdot \rho = v_1 \cdot A_1 \cdot \rho - \frac{v_1 \cdot A_1 \cdot \rho}{(n_f + 1) \cdot 2} \tag{14}$$

where:

v_{i-j} - Velocity in channel $i - j$; m/s

A_{i-j} - Cross-section area of channel $i - j$; m^2

n_f - Number of full sections (inner sections) in the assembly

As

$$A_1 = A_{3-5} = A_{5-7} = A_{7-9} = A_{9-11} = A_{11-13} = A_{13-15} = A_{15-17}$$

and ρ is constant:

$$v_{3-5} = v_1 - \frac{v_1}{(n_f + 1)\cdot 2} \tag{15}$$

The consecutive velocities were calculated as follows:

$$v_{i-j} = v_{m-i} - \frac{v_1}{(n_f + 1)} \tag{16}$$

where: "i" is an odd number between 5 and 15;

$j = i + 2$; and $m = i - 2$;

e.g. $v_{7-9} = v_{5-7} - \frac{v_1}{(n_f + 1)}$ (17)

As the velocities and consequently the flow rates in the vertical channels were known (13) the velocities along the top horizontal channel was calculated from the mass conservation equation.

In order to calculate appropriate flow resistance at each point of the distributing tube numbered in Fig. 11, the Bernoulli equation for each possible path of the water in the assembly was created, as shown below. The equations were created under the assumption that the velocity head in the bottom horizontal channel acted only in the horizontal direction, namely

$$h_{T1} - h_{T2} = \Delta h_{T3-5} + \Delta h_{T5-6} + \Delta h_{T6-4} + \frac{v_{3-5}^2}{2g} \tag{18}$$

where h_{T1} and h_{T2} are the total head at the points 1 and 2 consecutively;

Δh_{Ti-j} - Difference of total head between the points i and j;

g - Magnitude of gravitational acceleration

$$h_{T1} - h_{T2} = $$

$$= \Delta h_{T3-5} + \Delta h_{T5-7} + \Delta h_{T7-8} + \Delta h_{T8-6} + \Delta h_{T6-4} + \frac{v_{5-7}^2}{2g} \tag{19}$$

$$h_{T1} - h_{T2} = \Delta h_{T3-5} + \Delta h_{T5-7} + \Delta h_{T7-9} + \Delta h_{T9-10} + $$

$$+ \Delta h_{T10-8} + \Delta h_{T8-6} + \Delta h_{T6-4} + \frac{v_{7-9}^2}{2g} \tag{20}$$

$$h_{T1} - h_{T2} = $$

$$= \Delta h_{T3-5} + \Delta h_{T5-7} + \Delta h_{T7-9} + \Delta h_{T9-11} + \Delta h_{T11-12} + $$

$$+ \Delta h_{T12-10} + \Delta h_{T10-8} + \Delta h_{T8-6} + \Delta h_{T6-4} + \frac{v_{9-11}^2}{2g} \tag{21}$$

$$h_{T1} - h_{T2} = \Delta h_{T3-5} + \Delta h_{T5-7} + \Delta h_{T7-9} + \Delta h_{T9-11} + $$

$$+ \Delta h_{T11-13} + \Delta h_{T13-14} + \Delta h_{T14-12} + \Delta h_{T12-10}$$

$$+ \Delta h_{T10-8} + \Delta h_{T8-6} + \Delta h_{T6-4} + \frac{v_{11-13}^2}{2g} \tag{22}$$

$$h_{T1} - h_{T2} = \Delta h_{T3-5} + \Delta h_{T5-7} + \Delta h_{T7-9} + \Delta h_{T9-11} + $$

$$+ \Delta h_{T11-13} + \Delta h_{T13-15} + \Delta h_{T15-16} + \Delta h_{T16-14} + $$

$$+ \Delta h_{T14-12} + \Delta h_{T12-10} + \Delta h_{T10-8} + \Delta h_{T8-6} + $$

$$+ \Delta h_{T6-4} + \frac{v_{13-15}^2}{2g} \tag{23}$$

The flow resistance characteristics in the vertical channels (e.g. Δh_{T5-7}; Δh_{T14-12} was evaluated by means of the Fluent simulation of the flow through the channels (with constant flow rate along the channels). These characteristics (functions of the flow rate) were used in (18) - (23).

The vertical head losses were expressed as follows:

$$\Delta h_{T5-6} = \Delta h_{T\_casting} + \Delta h_{T\_screen\_5-6} \tag{24}$$

$$\Delta h_{T7-8} = \Delta h_{T\_casting} + \Delta h_{T\_screen\_7-8} \tag{25}$$

$$\Delta h_{T9-10} = \Delta h_{T\_casting} + \Delta h_{T\_screen\_9-10} \tag{26}$$

$$\Delta h_{T11-12} = \Delta h_{T\_casting} + \Delta h_{T\_screen\_11-12} \tag{27}$$

$$\Delta h_{T13-14} = \Delta h_{T\_casting} + \Delta h_{T\_screen\_13-14} \tag{28}$$

$$\Delta h_{T15-16} = \Delta h_{T\_casting} + \Delta h_{T\_screen\_15-16} \tag{29}$$

Where:

$\Delta h_{T\_casting}$ is the total head loss in a single casting with no distributing tube and it was calculated using data presented in Fig. 5.

$\Delta h_{T\_screen\_i-j}$ is the head loss produced by the part of the distributing tube under the *i-j* vertical channel.

As the flow rate of the water flowing through each casting is assumed to be the same, Δh_{T_screen} depends only on the diameter of holes in the distributing tube (because the

assumption was made that the head loss of the water flowing through the holes of the distributing tube depends only on the flow rate through the holes and the diameter of the holes).

The pressure drop caused by the perforated tube was calculated using Fluent for a fixed flow rate and various diameters of the holes in the distributing tube. Then an experimental orifice pressure drop formula [3] was rearranged and adapted in order to express the data provided by Fluent as an explicit function of the flow rate.

The experimental formula was rearranged as follows:

$$Q = C_0 A_{holes} \sqrt{\frac{2\Delta p}{\rho \cdot \left[1 - \left(\frac{A_{holes}}{A_{screen}}\right)^2\right]}} \tag{30}$$

$$\Delta p = \frac{Q^2 \cdot \rho \cdot \left[1 - \left(\frac{A_{holes}}{A_{screen}}\right)^2\right]}{2 \cdot C_0^2 \cdot A_{holes}^2} \tag{31}$$

The head loss Δh is defined as follows:

$$\Delta h = \frac{\Delta p}{\rho \cdot g} \tag{32}$$

Therefore:

$$\Delta h = \frac{Q^2 \cdot \left[1 - \left(\frac{A_{holes}}{A_{screen}}\right)^2\right]}{2 \cdot C_0^2 \cdot A_{holes}^2 \cdot g} = \frac{\left(A_{5-6} \cdot v_{5-6}\right)^2 \cdot \left[1 - \left(\frac{A_{holes}}{A_{screen}}\right)^2\right]}{2 \cdot C_0^2 \cdot A_{holes}^2 \cdot g} \tag{33}$$

where A_{screen} is the area of the piece of the screen (the distributing tube) including the holes which refer to one section of the heat exchanger assembly. A_{holes} is an area of the group of holes around the distributing tube referring to the particular section of the heat exchanger assembly. These groups are numbered in Fig. 11.

Q is a volumetric flow rate, $\frac{m^3}{s}$; C_0 is a discharge coefficient, dimensionless; g is the gravitational acceleration, $\frac{m}{s^2}$; Δp is a pressure drop, Pa; Δh is a head loss.

Then the discharge coefficient C_0 was chosen so that (33) matches the pressure drop characteristic calculated using the Fluent software and we found that $C_0 = 0.77$ gave the best result. The comparison between (33) and the CFD simulation is shown in Fig. 12. The good agreement between the two curves in the figure suggests that the orifice pressure drop formula may be successfully used in order to approximate a pressure drop characteristic of a perforated tube as long as the discharge coefficient is known.

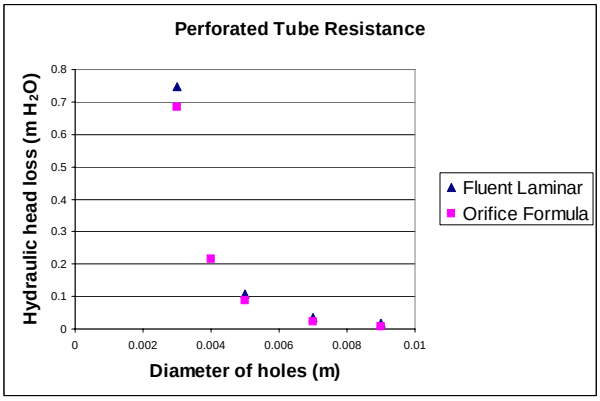

Fig. 12 Hydraulic head loss caused by the distributing tube calculated by (33) adapted to match the data derived using Fluent

Equation (13)÷ (29) and (33) were introduced to the MS Excel and the diameters of the holes in the distributing tube that satisfy these equations were calculated by means of the MS Excel solver.

As various configurations of the diameters of the holes in the distributing tube can give the uniform water distribution, a unique solution of the set of equations does not exist. Therefore additional input data is needed in order to produce a unique solution.

Therefore the diameter of the group of holes at the point 5 (see Fig. 10 and Fig. 11) was assumed to be known and calculations were performed for a few different values of this diameter.

The results obtained are presented in Fig. 13 and Fig. 14

Fig. 13 illustrates the calculated diameters of the holes in the distributing tube which refer to particular sections of the heat exchanger assembly for various assumed diameters of the holes at point 5.

Fig. 14 illustrates the dependence between the pressure drop in the entire assembly of the heat exchanger and the particular configuration of the holes in the distributing tube (each particular configuration refers to the specific diameter of the group of holes at point 5).

As described in [3], one of the possible ways to ensure a uniform distribution of the fluid-flow is to make the diameters of holes in the distributing tube uniform but small enough to produce large pressure drop compared to the pressure variation which causes maldistribution. Therefore if smaller holes were used then the water distribution would be expected to be better in the case of insufficient accuracy in the performed calculations.

The configuration of holes in the distributing tube which refers to the 5mm diameter of the group of holes at point 5 was chosen. That was because it gives a similar pressure drop in the entire assembly to that of the larger holes (see Fig. 14), but it was believed to give better water flow distribution in case of insufficient accuracy in the performed calculations as described above.

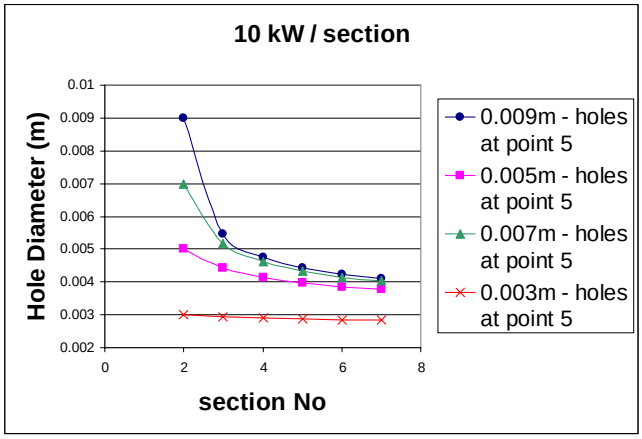

Fig. 13 Various configurations of diameter of holes in the distributing tube of the heat exchanger that should give a uniform water distribution.

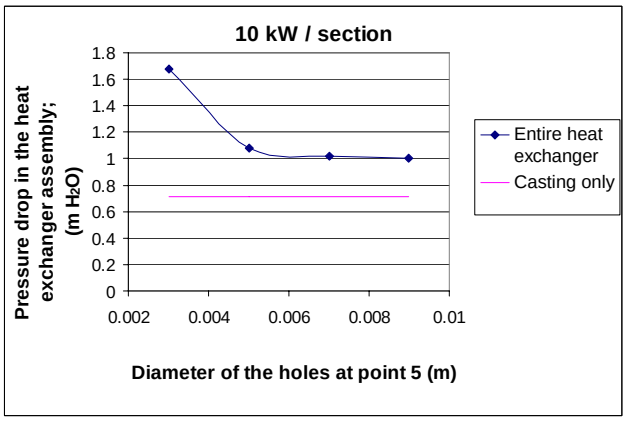

Fig. 14 Pressure drop in the entire assembly of the heat exchanger for various diameters of the second hole in the distributing tube

The selected final design configuration of the diameters of holes in the distributing tube is shown in Table I. As the production tolerance would be 0.2 mm then the results are rounded to 1 decimal place.

TABLE I
THE SELECTED FINAL CONFIGURATION OF DIAMETERS OF HOLES IN THE DISTRIBUTING TUBE OF THE HEAT EXCHANGER

Section No	diameter of holes; mm
1	5
2	5
3	4.4
4	4.1
5	4.0
6	3.8
7	3.8
8	3.8

VI. CONCLUSION

As shown in this paper, various approximations and simplifications can be made in order to decrease the time and computational resources needed for a CFD analysis. As the CFD analysis of the changed geometries of large systems (for optimisation purposes) is time consuming, some flow characteristics of particular elements of a system can be derived using CFD and utilised in the Bernoulli Equation for the flow optimisation problems.

Simple spread sheet calculations can quickly solve design optimisation problems which would be very difficult to solve by CFD alone in a reasonable time as it would be a trial and error process. On the other hand spread sheet calculations alone are not able to predict the flow resistance characteristic for an arbitrary geometry, where CFD may be very helpful.

However required approximations and assumptions in such an approach may lead to errors. Therefore some additional evaluations of the proposed design should be conducted. This might be a CFD simulation of the optimised design, ideally confirmed by measurements.

ACKNOWLEDGMENT

L. Peronski thanks the Knowledge Transfer Partnership (KTP) program for financial support.

REFERENCES

[1] General metrology - Part 4: Practical guide to measurement uncertainty (PD 6461-4:2004) British Standard Institution (BSI) 20 August 2004
[2] General metrology - Part 3: Guide to the expression of uncertainty in measurement (GUM) (PD 6461-4:2004) British Standard Institution (BSI) 13 June 2003 (page61);
[3] Perry, R.H., J. O. Maloney, D. W Green, *Perry's chemical engineers' handbook*. 7th ed. 1999, New York: McGraw-Hill. p. 6-21; p. 6-32 ÷ 6-34.
[4] Bejan, A., A.D. Kraus, and Knovel (Firm), *Heat transfer handbook*. 2003, J. Wiley: New York. p. xiv, 1480 p.
[5] Rohsenow, W.M., J.P. Hartnett, and Y.I. Cho, *Handbook of heat transfer*. 1997, McGraw-Hill: London. p. 1600p.
[6] Kays, W.M. and A.L. London, *Compact heat exchangers*. 3rd ed. 1998, Malabar, Florida: Krieger Publishing Company. 335p.
[7] Sahin, H.M., A.R. Dal, and E. Baysal, *3-D Numerical study on the correlation between variable inclined fin angles and thermal behavior in plate fin-tube heat exchanger*. Applied Thermal Engineering, 2007. 27(11-12): p. 1806-1816.
[8] Taler, D., *Determination of heat transfer correlations for plate-fin-and-tube heat exchangers*. Heat and Mass Transfer, 2004. Volume 40(10).
[9] Erek, A., B. Ozerdem, L. Billir, Z. Ilken, *Effect of geometrical parameters on heat transfer and pressure drop characteristics of plate fin and tube heat exchangers*. Applied Thermal Engineering, 2005. 25(14-15): p. 2421-2431
[10] Sundén, B., *Computational Fluid Dynamics in Research and Design of Heat Exchangers*. Heat Transfer Engineering, 2007. 28(11): p. 898 - 910.
[11] Fluent 6.2 User's Guide section 7.19.6; 7.19.2